

- (1981).
 11. M. L. Lappert and S. J. Miles, *J. Organomet. Chem.*, **212**, C4 (1981).
 12. Y. Sasson and G. L. Rempel, *Tetrahedron Lett.*, 3221 (1974).

Infrared Multiphoton Dissociation of CF₂HCl: Laser Fluence Dependence and the Effect of Intermolecular Collisions

Nam Woong Song, Kook Joe Shin, Sangyoub Lee,
Kyung-Hoon Jung[†], Kwang Yul Choo[‡], and Seong Keun Kim*

Department of Chemistry, Seoul National University, Seoul 151-742

[†]*Department of Chemistry, Korea Advanced Institute of Science and Technology, Seoul 130-650*

Received June 3, 1991

The effect of intermolecular collisions in the infrared multiphoton dissociation (IRMPD) of difluorochloromethane was investigated using He, Ar, and N₂ as buffer gases. The reaction probability for IRMPD of difluorochloromethane was measured as a function of laser fluence and the buffer gas pressure under unfocused beam geometry. It was observed that the reaction probability was initially enhanced with the increase of buffer gas pressure up to about 20 torr, but showed a decline at higher pressures. The reaction probability increases monotonically with the laser fluence, but the rate of increase diminishes at higher fluences. An attempt was made to simulate the experimental results by the method of energy grained master equation (EGME). From the parameters that fit the experimental data, the average energy loss per collision, $\langle \Delta E \rangle_d$, was estimated for the He, Ar, and N₂ buffer gases.

Introduction

An intense, pulsed IR laser radiation has been shown to promote molecules in the gas phase to high vibrational levels of the ground electronic state *via* the simultaneous absorption of many infrared photons. It is now well established that when a molecule is excited above a certain level by IR multiphoton absorption (IRMPA), the energy pumped into the molecule is more or less randomly distributed among all vibrational degrees of freedom before decomposition starts.¹⁻⁶ Such a highly excited molecule is not qualitatively very different from the energized molecules or transient complexes produced by inelastic and/or reactive molecular collisions, and the IRMPD technique has been widely used for the study of dynamics of unimolecular reactions.

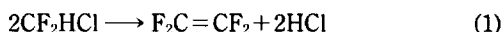
Since the first report of IRMPD of CF₂HCl,⁷ many studies have been done on the IR laser induced chemistry of this molecule. Grunwald *et al.* reported the effect of buffer gas pressure on the macroscopic absorption cross section and the dissociation yield.⁷ Sudboe *et al.* investigated the three-center unimolecular elimination reaction of HCl from CF₂HCl in a molecular beam experiment, and showed that the measured translational energy distribution of the product could be explained by the statistical (RRKM) theory.^{8,9} Stephenson *et al.* studied the laser intensity and Ar pressure dependence of IRMPD of CF₂HCl by monitoring the CF₂: (\bar{X}^1A_1) carbene with the laser-induced fluorescence technique.¹⁰⁻¹³ They re-

ported that there existed a narrow "linear dependence" range in the log-log plot of dissociation probability *vs.* laser fluence between 5-25 MW/cm² of laser intensity; a smooth bending over and saturation in product formation was also observed (25-150 MW/cm²). Increasing Ar pressure above a certain level (~50 torr) initially increased the CF₂HCl dissociation rate due to what may be called the "rotational hole-filling", but the rate soon became independent of Ar pressure up to 1 atm. They were also able to reproduce their results by a model calculation. Van den Bergh *et al.* reported a different pressure dependence feature in the IRMPD of CF₂HCl.¹⁴⁻¹⁶ They used unfocussed laser pulses (2-8 J/cm²) and observed the collisional deactivation effect of Ar buffer gas. They tried to simulate the results with a model calculation, and found that simple energy-grained master equation (EGME) was adequate to describe the IRMPD results of CF₂HCl.¹⁴⁻¹⁶ Dolikov *et al.* examined the possibility of mode-selectivity of multiphoton excitation, but they found it impossible to excite a specific mode at least on the time scale of 10⁻⁸ sec. They observed that absorption of mere 4-5 quanta resulted in the excitation of all vibrational modes.⁶

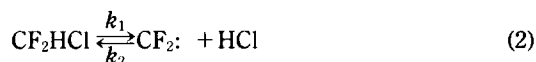
Recent studies of the IRMPD of CF₂HCl include subjects such as deuterium separation using the difference of absorption cross section due to the isotope effect,¹⁷ the effect of laser frequency and translational energy on the IRMPD of CF₂HCl,¹⁸ and CF₂: carbene generation for the purpose of secondary use in bimolecular reaction chemistry with diatomic molecules.^{19,20}

The laser-induced reaction of this molecule is particularly simple, being represented by

[†]Deceased.



No product other than C₂F₄ and HCl was detected. These products are identical with those obtained in homogeneous gas-phase pyrolysis,²¹ whose kinetics and thermochemistry are consistent with the following two-step mechanism.



Dissociation (rate constant k_1) is rate determining, with a limiting high-pressure activation energy of 55.9 kcal/mol.²¹ As HCl accumulates, reaction of CF₂ with HCl (rate constant k_2) is expected to compete effectively with reaction 3. Under our experimental conditions, it can be shown that the rate of reverse reaction in Eq. (2) is much smaller than the forward reaction rate in Eq. (3), so that only the forward reaction is important in Eq. (2).

We have investigated the fluence dependence of IRMPD of CF₂HCl at fixed pressures (30 and 70 torr) of several buffer gases. The pressure dependence was also examined by varying the buffer gas pressure in 0-90 torr range. Different buffer gases are expected to have varying degrees of efficiency toward collisional deactivation of target molecule. Generally, it is believed that the collisional deactivation efficiency increases as the mass and complexity or number of degrees of freedom of buffer gas increase.

An attempt was made in the present study to compare three different inert gases He, Ar, and N₂ in their efficiencies toward collisional deactivation.

The experimental results were compared with a theoretical calculation based on the EGME model. From the parameters that fit the experimental results, the average energy loss per collision, $\langle \Delta E \rangle_d$, was evaluated for the He, Ar, and N₂ gases.

Experimental

Materials. Gaseous CF₂HCl (>99.9%) was obtained from Aldrich Chemical Co. It was analyzed by a gas chromatograph and found to be free of detectable impurities. The gas was handled on a vacuum line by standard techniques and degassed before each run by freeze-pump-thaw cycles. The amount of the sample was measured by the MKS Baratron 0-1 torr pressure transducer.

Buffer gases He, Ar, and N₂ (>99.99%) were obtained from Matheson Co. and were used without further purification. The pressure of the gases was monitored by the MKS Baratron 0-100 torr pressure transducer.

Apparatus and Procedure. A detailed description of the apparatus has been given elsewhere.²² A TEA CO₂ laser (Tachisto 215G) was used as an excitation source. The laser pulse consists of a 40 nsec (FWHM) gain switched spike and a low intensity tail of 500 nsec. The irradiation line, R(32) 1086 cm⁻¹, is in resonance with CF₂ antisymmetric stretching vibration. The effective molar extinction coefficient at the maximum near 1116 cm⁻¹ has been reported to be $(7.1 \pm 0.1) \times 10^5$ cm²mol⁻¹.¹⁴ To provide a more homogeneous laser beam, the beam size was reduced by an iris diaphragm.

The diameter of the beam was determined from burn patterns on a heat sensitive paper. Laser output fluence was varied by attenuating the incident beam with polystyrene films. The laser pulse energy was measured with a calorimeter (Scientech 36-2001). Pulse to pulse stability was $\pm 3\%$. The unfocused beam (7 mm in diameter) was passed through the reaction cell (10 cm long, 2 cm inner diameter) fitted with NaCl windows. The reflected or absorbed energy of the laser radiation by the inlet window was calibrated. It was found that ca. 92% of the total incident energy was transmitted through the inlet window.

The dissociation measurements were carried out at a constant sample partial pressure of 0.5 torr. To obtain quantities sufficient for our detection scheme, the products were accumulated for 100-500 laser shots at 1 pps repetition rate, keeping the fraction of undissociated reactant above 70%.

The reaction yield was measured by a gas chromatograph (Yanaco G-80) with an FID detector. A Hall M-18-OL column of 2×2.4 m length was used.

Results and Discussion

Justification of Neglecting the Reverse Reaction in Eq. (2). The dissociation probability at a given laser fluence and buffer gas pressure, $P(\Phi)$, is defined as the number of molecules in the irradiated volume that react per pulse divided by the total number of molecules in the irradiated volume. $P(\Phi)$ was calculated from Eq. (4), whose derivation is given in the Appendix.

$$P(\Phi) = (V_T/V_{ir})[1 - (C_i/C_0)^{1/i}] \quad (4)$$

V_T : total volume of the reaction cell

V_{ir} : the irradiated volume

C_0 : the concentration of reactant before irradiation

C_i : the concentration of reactant after i -th irradiation

i : the number of irradiated pulses

To determine the unimolecular dissociation rate by monitoring the decreased reactant concentration or the increased product concentration, we have to make sure that the backward reaction rate in Eq. (2) is negligible compared with the forward reaction rate in Eq. (3). We measured the total dissociation yield of the reaction mixture CF₂HCl-HCl by varying only the HCl pressure over 0.2-1 torr range. N₂ gas of 30 torr was added to reduce the collisional effect of HCl. The results are given in Figure 1, which shows the product yield is not affected by the increase of HCl pressure up to 1 torr. Since the dissociation measurements were carried out at a constant reactant pressure of 0.5 torr which would result in 0.5 torr HCl at most, the above results indicate that backward reaction to reactant is negligible under our experimental conditions. Thus measurements of the final product concentrations yield direct measure of unimolecular dissociation rates.

Effect of Intermolecular Collisions. The dissociation probability for the IRMPD of CF₂HCl was measured as a function of buffer gas pressure at 0.32 J/pulse of laser energy. Three different inert gases, He, Ar, and N₂, were used as the buffer gas. The pressure of the reactant, CF₂HCl, was kept constant at 0.5 torr in all runs.

The variation of $P(\Phi)$ with buffer gas pressure is re-

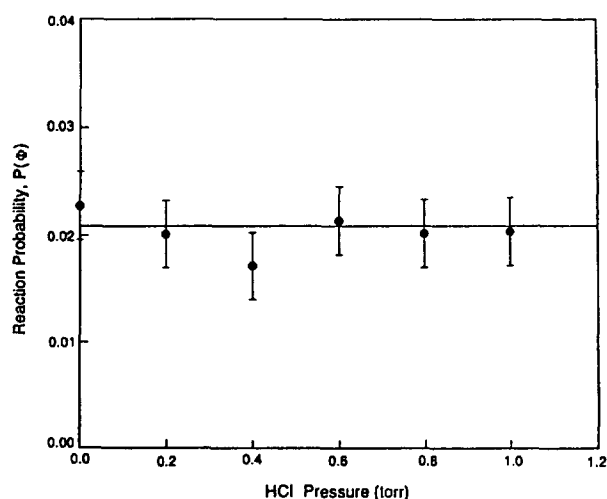


Figure 1. The plot of reaction probability *vs.* pressure of added HCl at 0.32 J/pulse.

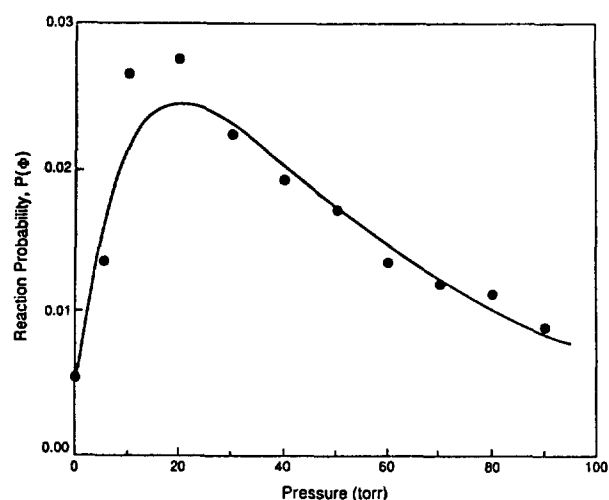


Figure 2. The plot of reaction probability *vs.* pressure of added He at 0.32 J/pulse. The points (•) are the experimental results. The solid curve represents the best fit results with $\langle \Delta E \rangle_d = 0.98$ Kcal/mol.

presentatively shown in Figure 2 for He. Data for other gases are tabulated in Table 1. In all cases, it is observed that adding a small amount of the collider gas up to 20 torr enhances the dissociation probability, while further increase impedes the reaction.

This trend in the variation of the reaction rate with the buffer gas pressure reveals that two conflicting types of collisional mechanisms are involved: the rotational hole-filling *vs.* the collisional deactivation.^{11,23} The weak perturbations introduced by the collider gas at lower pressures not only induce the collisional coupling of previously uncoupled states, but also bring about efficient $T \leftrightarrow R$ energy transfer to compensate for the mismatch in energy between the laser photon and the vibrational anharmonicity. This leads to the enhancement in the dissociation rate.

Rotational states are the ones that are initially coupled by collisions, but as the pressure is raised vibrational states are couple as well, hence opening collisional deactivation

Table 1. The Dependence of Dissociation Probability of CF_2HCl on Buffer Gas Pressure

Pressure of added buffer gas (torr)	Dissociation probability $P(\Phi) (\times 10^2)$		
	He	Ar	N_2
0.00	0.550	0.550	0.550
5.00	1.42	1.35	1.87
10.0	2.10	2.66	2.68
20.0	2.76	2.65	2.81
30.0	2.25	2.13	2.29
40.0	1.93	2.04	1.61
50.0	1.71	1.88	1.18
60.0	1.34	1.45	1.22
70.0	1.18	1.43	1.06
80.0	1.11	1.31	0.761
90.0	0.882	0.886	0.670

* Reactant pressure: 0.5 torr. * Pulse energy: 0.32 J. * Number of irradiated pulses: 100-500.

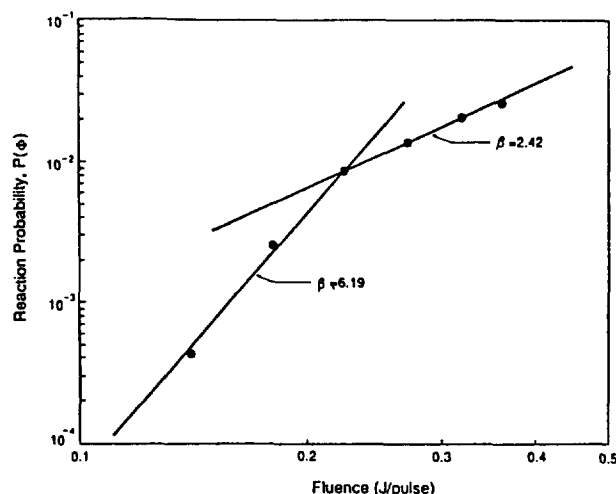


Figure 3. The plot of reaction probability *vs.* laser fluence with added Ar gas of 30 torr. The points (•) are the experimental results. The slope of the solid lines is the exponent for the power law dependence of dissociation probability on laser fluence, i.e. $P(\Phi) \sim \Phi^\beta$.

channels due to $V \rightarrow T$ energy transfer. As the collider gas pressure is further raised, increased collision frequency make the usually inefficient $V \rightarrow T$ energy transfer occur at such rate that the latter starts to compete effectively with the multiphoton pumping process. At sufficiently high pressures, collisional deactivation of the vibrationally excited reactants predominates over the multiphoton pumping so that the overall dissociation rate drops.

Laser Fluence Dependence of the Reaction Rate.

The dissociation yield in IRMPD of 0.5 torr CF_2HCl was measured as a function of fluence under constant pressure. The results are represented in Table 2 and Figures 3-5.

As shown in Figure 3, the slope of the $\log P(\Phi)$ *vs.* $\log \Phi$ curve decreases as the laser fluence (Φ) is increased. This is a feature frequently observed in the IRMPD experi-

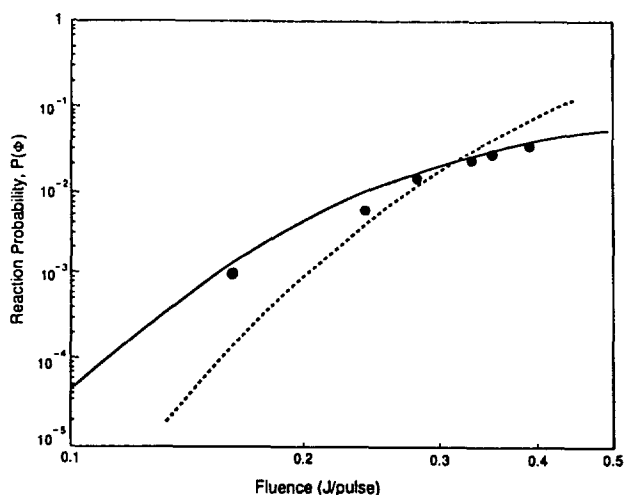
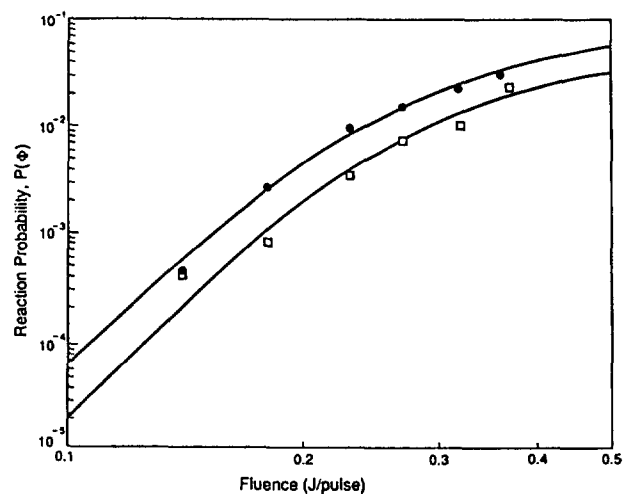
Table 2. The Dependence of Dissociation Probability of CF_2HCl (0.5 torr) on Laser Fluence

a) with He buffer gas		
Pressure of added He gas (torr)	Energy per pulse (J/pulse)	Dissociation probability $P(\Phi) (\times 10^2)$
30.0	0.39	3.33
	0.35	2.57
	0.33	2.09
	0.28	1.32
	0.24	0.569
	0.16	0.096
70.0	0.39	2.75
	0.32	1.18
	0.27	0.789
	0.22	0.442
	0.15	0.055

b) with Ar buffer gas		
Pressure of added Ar gas (torr)	Energy per pulse (J/pulse)	Dissociation probability $P(\Phi) (\times 10^2)$
30.0	0.36	2.74
	0.32	2.13
	0.27	1.43
	0.23	0.926
	0.18	0.256
	0.14	0.043
70.0	0.37	2.14
	0.32	0.955
	0.27	0.683
	0.22	0.323
	0.16	0.081
	0.14	0.039

c) with N_2 buffer gas		
Pressure of added N_2 gas (torr)	Energy per pulse (J/pulse)	Dissociation probability $P(\Phi) (\times 10^2)$
30.0	0.38	2.97
	0.32	2.29
	0.27	1.04
	0.23	0.348
	0.17	0.118
70.0	0.38	2.49
	0.34	1.19
	0.32	1.06
	0.27	0.517
	0.22	0.240
	0.16	0.072

ments under mildly focusing condition.^{24,25} In IRMPD experiments, $P(\Phi)$ typically exhibits a power-law dependence on laser fluence, i.e. $P(\Phi) \propto \Phi^\beta$. Under focusing geometry, the value of β is usually *ca.* 1.5,^{28,29} but in experiments using

**Figure 4.** The plot of reaction probability *vs.* laser fluence with added He gas of 30 torr. The points (•) are the experimental results. The solid curve represents the best fit results with the function $f(\Phi)$. The dashed curve represents the results without the function $f(\Phi)$, as in van den Bergh *et al.*'s study.**Figure 5.** The plot of reaction probability *vs.* laser fluence with added Ar gas. (•) 30 torr, (□) 70 torr of Ar. The solid curve represents the best fit results with the function $f(\Phi)$.

low energy pulses, the reported values of β range from 4 to 6.²⁴⁻²⁷

Our data shows two distinct types of $P(\Phi)$ dependence on laser fluence. As shown in Figure 3, the values of β in the high and low fluence regions are *ca.* 2.4 and 6.2, respectively. The "saturation" behavior at high fluence region is a result of depleting the population of low-lying pumpable states with higher laser fluence. It is expected that the saturation should start at a lower fluence level as the pressure is decreased since the collisional $V \rightarrow T$ energy transfer would become too slow to replenish the depleted low-lying states. However, in the limited ranges of pressure and fluence in our experiments, we were not able to observe such effect.

Model Calculation. In order to extract more quantitative information not available directly from experiments, a numerical analysis based on a theoretical model has been

carried out. We have modeled the pressure and fluence dependence of the multiphoton dissociation of CF_2HCl by using the energy-grained master equation (EGME), which is a set of coupled differential equations describing the rate of change in the molecular populations between adjacent energy levels separated by ΔE .

The differential equations used to fit the IRMPD data of CF_2HCl are as follows:

$$\begin{aligned} dN_i/dt &= R_{i-1}^a N_{i-1} + R_i^e N_{i+1} - (R_i^a + R_{i-1}^e) N_i \\ &\quad + \sum_j Z P_{ij} N_j - \sum_j Z P_{ji} N_i - k_i N_i; \quad i \geq 1. \\ dN_{p_0}/dt &= R_0^a N_1 - R_0^e N_{p_0} + \sum_j Z P_{p_0 j} N_j - \sum_j Z P_{j p_0} N_{p_0} + (1/\tau_{rot}) N_{n_0} \\ dN_{n_0}/dt &= -(1/\tau_{rot}) N_{n_0} \end{aligned} \quad (5)$$

Here, the various symbols have the following meanings:

N_i : the population in level i

R_i^a : the rate coefficient for absorption from level i to $i+1$.

R_i^e : the rate coefficient for stimulated emission from level $i+1$ to i .

Z : the hard sphere collision frequency

P_{ij} : the probability of transition from level j to level i by single collision.

N_{p_0} : the population of ground vibrational state which is pumpable by laser radiation

N_{n_0} : the population of non-pumpable ground vibrational state

τ_{rot} : the rotational relaxation time

k_i : the dissociation rate constant from level i .

The above differential equations were solved by numerical integration using the Burlish-Stoer procedure.³⁰ The integration of the equations started from the time for "laser on" and continued until the undissociated molecular populations above the threshold energy level were less than 5% of the dissociated molecular population. The time increment in the integrating step was taken to be 1/1000 of the pulse duration of laser. The level separation was normally taken to be the laser single photon energy, $h\nu = 1086 \text{ cm}^{-1}$ or 3.09 kcal/mol.

The absorption rate coefficient was modified from van den Bergh *et al.*'s formula¹⁶ to have:

$$\begin{aligned} R_i^a &= \sigma_i I(t) f(\Phi) / h\nu \\ f(\Phi) &= 1.72 \exp(-1.7 \Phi) \end{aligned} \quad (6)$$

where σ_i is the effective absorption cross section for transition from level i to $i+1$, $I(t)$ is the laser intensity, and $h\nu$ the photon energy. $f(\Phi)$ is a parametric function employed to describe the increasing importance of the anharmonic bottleneck effect with the increase of fluence.³¹

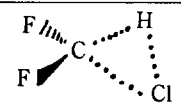
The stimulated emission rate may then be determined from detailed balancing:

$$R_i^e = R_i^a (g_i / g_{i+1}) \quad (7)$$

where g_i is the number of vibrational states within the laser bandwidth centered at the energy $i h\nu$. For narrow laser lines, g_i is proportional to the density of vibrational states at energy E_i .

$$g_i / g_{i+1} = \rho_i / \rho_{i+1} \quad (8)$$

Table 3. Input Parameters for RRKM Calculation

Molecule	Activated complex	
CF_2HCl		
mode	Vibrational frequencies in cm^{-1}	
ν_1	3025	3025
ν_2	1311	1500
ν_3	1178	1178
ν_4	809	1116
ν_5	595	595
ν_6	422	500
ν_7	1347	1600
ν_8	1116	1600
ν_9	365	1000
$I_a I_b I_c$	3.96×10^6	2.47×10^6
Other parameters		
$\log A$	12.6	
E_0	56	
L^+	1	

* Vibrational frequencies of the molecule and the complex are taken from Ref. (8). * $I_a I_b I_c$: The product of the moments of inertia ($\times 10^{-120} \text{ g}^3 \text{cm}^6$). * L^+ : Reaction path degeneracy.

The densities of vibrational states and the rate constants, k_i 's, were calculated by Whitten-Rabinovitch method and RRKM theory, respectively. k_i 's were set equal to zero when the energy of the excited molecule was lower than the activation energy. Vibrational frequencies of the reactant and the complex were taken from Ref. 8. Moments of inertia of the reactant and the complex were calculated based on the geometries obtained from MNDO calculations.

The time dependence of the laser intensity, $I(t)$, was represented by approximating the true laser pulse as a parameterized rectangular pulse. From the shape of the temporal profile of the actual laser pulse, both 40 nsec and 60 nsec rectangular pulses, each containing 70 and 30% of the total pulse energy, were used.³² The laser intensity was then determined for the assumed pulse shape with a beam diameter of 7 mm and a total energy equal to the experimentally determined value.

The level-dependent absorption cross-section, σ_i , was assumed to vary in the following way²³:

$$\sigma_i = \sigma_0 (i+1)^{-n} \quad (9)$$

where σ_0 is the absorption cross-section for ground vibrational state, and n is an adjustable parameter that takes into account the variation of the absorption cross-sections with vibrational excitation of the molecule. The value of the absorption cross-section for ground state was taken as $1.18 \times 10^{-18} \text{ cm}^2$, which is the experimental value reported by van den Bergh *et al.*¹⁴

To determine the collisional transition probability, P_{ij} , the exponential gap model was used.²³ Collision diameters for He, Ar and N_2 were obtained from previous works.³³ These

were 2.6, 3.4 and 3.7 Å, respectively. The collision diameter of CF₂HCl was estimated to be 4.9 Å by comparison with CHCl₃ (5.5 Å), and CHF₃ (4.56 Å).^{34,35}

Finally, $1/\tau_{rot}$ was initially taken to be equal to the collision frequency due to the lack of data on rotational relaxation for CF₂HCl.

The results calculated from the EGME model were fitted to the experimental data using an iterative fitting procedure in which the following parameters were adjusted: n , N_{p0} , $1/\tau_{rot}$, $f(\Phi)$ and $\langle\Delta E\rangle_d$, the average energy loss per collision.

The pressure dependence data were fitted first. To obtain a reasonable fit for the result, a series of calculations were carried out in which two of N_{p0} , $\langle\Delta E\rangle_d$, and $1/\tau_{rot}$ were kept constant and the third one varied. Such a procedure was repeated until a set of reasonable parameters that fits all of the pressure data was obtained. A major constraint in this fitting procedure was that N_{p0} and n should be the same for each set of pressure dependence data, since these parameters do not depend on the properties of the buffer gases.

After obtaining the best fits for the pressure dependence, the fluence data were simulated by introducing the parametric function $f(\Phi)$, while keeping the other four parameters (n , N_{p0} , $\langle\Delta E\rangle_d$, and $1/\tau_{rot}$) fixed. The fluence dependence data reasonably fitted with a unique parametric function.

Comparison with Experimental Results. The optimized results for the dependence of dissociation probability on the buffer gas pressure are shown as a solid curve in Figure 2. The fraction of pumpable states under collision-free condition was determined to be 5% by iterative fitting. The value of n was determined to be 0.35. With the parametric function, $f(\Phi)$, and $n=0.35$, the laser fluence dependence of the reaction probability was reasonably fitted. (Figure 4, 5)

It turned out that multiplying the collision frequency by 0.25 for He, 0.55 for Ar, and 0.50 for N₂ yielded the best fitting parameter for $1/\tau_{rot}$ (rotational relaxation rate) in each case. This confirms the intuitive notion that He is the least efficient collision partner for collisional relaxation of rotational motion of CF₂HCl.

The average energy transferred by a single collision, $\langle\Delta E\rangle_d$, which gave the best fits for the experimental data was 0.98 kcal/mol for He, 1.27 kcal/mol for Ar, and 1.25 kcal/mol for N₂ respectively. A similar pressure dependence data, but different deactivation energy were obtained by van den Bergh *et al.* They reported that $\langle\Delta E\rangle_d$ for Ar was about 0.1 kcal/mol, while our calculation obtained 1.27 kcal/mol. This large difference is mainly due to adoption of different procedures in treating the collisional effects in the model calculation. They excluded the rotational hole-filling effect and took into account only the deactivating effect of collisions. They obtained the collision-free dissociation yield from extrapolation of pressure dependence data (see ref. 16), and used it for the EGME calculation. It is expected that such data have a limited applicability in the fluence dependence of collisionless IRMPD, free from rotational hole-filling effect. The model we adopted deals with both aspects of collisions: rotational hole-filling and collisional deactivation; and it enables us to properly reproduce the data in which the product yield increases at the beginning of pressure rise and decreases thereafter due to predominant effect of collisional deactivation over rotational hole-filling.

In order for the deactivation to compete effectively with rotational hole-filling, $\langle\Delta E\rangle_d$ must not be so small. For example, calculation based on our model with $\langle\Delta E\rangle_d$ values of Ar smaller than 0.7 kcal/mol showed no decrease in product yield with the rise of buffer gas pressure. This is not very surprising since there will be only 10-15 collisions within laser pulse duration of 40 nsec. Even if every collision were effective, which obviously is very unlikely, $\langle\Delta E\rangle_d$ should be at least 0.2-0.3 kcal/mol in order to deactivate the molecule from $v=1$ to $v=0$ state.

Previous experiments revealed that $\langle\Delta E\rangle_d$ varied between 0.1-1.4 kcal/mol for He, 0.1-4.0 kcal/mol for Ar, and 0.3-4.0 kcal/mol for N₂.^{23,35-42} It is generally known that the deactivation efficiency increases as the size and complexity of buffer gases increase. Thus $\langle\Delta E\rangle_d$ for Ar may have been expected to be somewhat smaller than $\langle\Delta E\rangle_d$ for N₂.

In our experiment the three buffer gases were found to have not much different values of $\langle\Delta E\rangle_d$. According to Heymann *et al.*, Ar is a more efficient deactivating third body than N₂ in the UV photoisomerization of cycloheptatriene.³⁶ Apparently the deactivating efficiency seems to depend not only on the buffer gas but also on the energized molecule and the specific process involved.

Acknowledgement. This work was supported by the Basic Science Research Institute Program, Ministry of Education, 1990, Project No. BSRI-90-311.

Appendix. Derivation of the equation for the dissociation probability from concentration measurement.

Let α and P_i be the dissociation probability and the concentration of the product molecules produced by the i -th laser pulse, respectively.

$$\text{Then } P_1 = C_0\alpha, \text{ and } C_1 = C_0 - P_1 = C_0(1 - \alpha).$$

$$\text{Likewise, } P_i = C_{i-1}\alpha = C_0(1 - \alpha)^{i-1}\alpha \quad (i \geq 2)$$

$$\text{and } C_i = C_{i-1} - P_i \\ = C_0(1 - \alpha)^i \quad (i \geq 0)$$

$$\text{Thus, } \alpha = 1 - (C_i/C_0)^{1/i}$$

Since one irradiates only a small volume (V_{ir}) with laser but monitors the concentration change in the whole volume (V_T), one has to make a correction to obtain $P(\Phi)$;

$$P(\Phi) = (V_T/V_{ir})\alpha = (V_T/V_{ir})[1 - (C_i/C_0)^{1/i}].$$

References

1. N. Isenor and M. C. Richardson, *Appl. Phys. Letts.*, **18**, 224 (1971).
2. N. Isenor, V. Merchant, R. Hallsworth, and M. Richardson, *Can. J. Phys.*, **51**, 1281 (1973).
3. A. S. Sudboe, P. A. Schulz, Y. T. Lee, and Y. R. Shen, *J. Chem. Phys.*, **68**, 1306 (1972).
4. J. Oref and B. S. Rabinovitch, *J. Phys. Chem.*, **81**, 2587 (1977).
5. R. Kadibelban, R. Ahrens-Botzong, and P. Hess, *Z. Naturforsch.*, **37**, 271 (1982).
6. V. S. Malinovsky, and Y. S. Doljnikov, V. S. Letokhov, A. A. Makarov, A. L. Malinovsky, and E. A. Ryabov, *Chem. Phys.*, **102**, 155 (1986).
7. E. Grunwald, K. J. Olszyna, D. F. Dever, and B. Knishkowsky, *J. Chem. Soc.*, **99**, 6515 (1977).

8. A. S. Sudboe, P. A. Schulz, Y. R. Shen, and Y. T. Lee, *J. Chem. Phys.*, **69**, 2312 (1978).
9. A. S. Sudboe, P. A. Schulz, Y. R. Shen, and Y. T. Lee, *Top. Curr. Phys.*, **35**, 95 (1986).
10. J. C. Stephenson and D. S. King, *J. Chem. Phys.*, **69**, 1485 (1978).
11. J. C. Stephenson, D. S. King, M. F. Goodman, and J. Stone, *J. Chem. Phys.*, **70**, 4496 (1979).
12. J. C. Stephenson and D. S. King, *Chem. Phys. Lett.*, **66**, 33 (1979).
13. J. C. Stephenson, J. A. Blazy, C. L. Li, and D. S. King, *J. Chem. Phys.*, **76**, 5989 (1982).
14. R. Dupperex and H. van den Bergh, *Chem. Phys.*, **71**, 3613 (1979).
15. R. Dupperex and H. van den Bergh, *J. Chem. Phys.*, **73**, 585 (1980).
16. A. C. Baldwin and H. van den Bergh, *J. Chem. Phys.*, **74**, 1012 (1981).
17. J. Moser, P. Morand, R. Dupperex, and H. van den Bergh, *Chem. Phys.*, **79**, 277 (1983).
18. R. N. Zitter, D. F. Koster, and H. K. Yun, *Optics Comm.*, **63**, 409 (1987).
19. C. Ungureanu, *Rev. Roum. Phys.*, **32**, 321 (1987).
20. N. Taisuke, T. Harutoshi, and M. Chi, *Chem. Phys. Lett.*, **134**, 347 (1987).
21. R. G. Barnes, R. A. Cox, and R. F. Simmons, *J. Chem. Soc. B.*, 1176 (1971).
22. B. S. Chun, N. W. Song, and K. Y. Choo *Bull. Kor. Chem. Soc.*, **11**, 214 (1990).
23. W. A. Jalenak and N. S. Nogar, *J. Chem. Phys.*, **79**, 816 (1983).
24. (a) S. Kato, Y. Makide, T. Tominaga, and K. Tacheuchi, *J. Phys. Chem.*, **88**, 3977 (1984); (b) S. Kato, Y. Makide, T. Tominaga, and K. Tacheuchi, *J. Phys. Chem.*, **91**, 4278 (1978).
25. (a) P. K. Chowdhury, K. V. S. Rama Rao, and J. P. Mittal, *J. Phys. Chem.*, **90**, 2877 (1986); (b) P. K. Chowdhury, K. V. S. Rama Rao, and J. P. Mittal, *J. Phys. Chem.*, **92**, 102 (1988).
26. D. W. Setser, T. S. Lee, and W. C. Danen, *J. Phys. Chem.*, **89**, 5799 (1985).
27. W. C. Danen, V. C. Rio, and D. W. Setser, *J. Am. Chem. Soc.*, **104**, 5431 (1982).
28. J. L. Lyman, S. D. Rockwood and S. M. Freund, *J. Chem. Phys.*, **67**, 4545 (1977).
29. M. Gauthier, P. A. Hacket, and C. Willis, *Chem. Phys.*, **45**, 39 (1980).
30. J. R. Rice, ed., "Mathematical software"; Academic Press; New York, 1971.
31. M. L. Azcarate, E. J. Quel, B. Toselli, J. C. Ferrero, and E. H. Staricco, *J. Phys. Chem.*, **92**, 403 (1988).
32. S. H. Kim, *M. S. Thesis*, Seoul Nat'l Univ. (1989).
33. J. O. Herschfelder, C. F. Curties, and R. B. Bird, ed., "Molecular Theory of Gases and Liquids"; New York, 1954.
34. F. Magnotta and I. P. Herman, *J. Chem. Phys.*, **81**, 2363 (1984).
35. J. E. Baggott and D. W. Law, *J. Chem. Phys.*, **85**, 6475 (1986).
36. M. Heymann, H. Hippler, and J. Troe, *J. Chem. Phys.*, **80**, 1853 (1984).
37. D. C. Tardy and B. S. Rabinovitch, *J. Chem. Phys.*, **48**, 5194 (1968).
38. D. W. Setser and E. E. Siefert, *J. Chem. Phys.*, **57**, 3623 (1972).
39. Y. Langsam and A. M. Ronn, *J. Chem. Phys.*, **80**, 749 (1984).
40. J. R. Barker, *J. Phys. Chem.*, **88**, 11 (1984).
41. H. Hippler, L. Lindemann, and J. Troe, *J. Chem. Phys.*, **83**, 3906 (1985).
42. V. V. Krongauz, B. S. Rabinovitch, and E. Linkaityte-Weiss, *J. Chem. Phys.*, **78**, 5643 (1983).

Theoretical Studies on the Gas-Phase Nucleophilic Aromatic Substitution Reaction¹

Ikchoon Lee*, Hyoung Yeon Park, and Bon-Su Lee

Department of Chemistry, Inha University, Incheon 402-751. Received July 18, 1991

The gas-phase nucleophilic substitution reaction of pentafluoroanisole with OH⁻ and NH₂⁻ nucleophiles have been studied theoretically using the AM1 method. Three reaction channels, S_N2, IPSO and S_NAr (scheme 1), are all very exothermic so that all are accessible despite the varying central energy barriers which are much lower than the reactants level. In the IPSO and S_NAr channels, the reactants form directly a stable σ-anion complex which proceeds to form a proton transfer complex *via* a transition barrier corresponding to a loose π-type complex with the F⁻ (or OCH₃⁻) leaving group. Due to a greater number of probable reaction sites available for S_NAr compared to the other two processes, the S_NAr channel is favored as experimentally observed.

Introduction

Nucleophilic aromatic substitution reactions²⁻⁷ have been

studied extensively in solution.⁸ The reactions proceed via the addition-elimination pathway (the S_NAr mechanism)⁹ and are normally rationalized by postulation of anion σ complexes